A Linear, Four-Spin Mn(II)−Nitronyl−Nitroxide-Substituted Phosphine Oxide System Exhibiting Both Antiferro- and Ferromagnetic Interactions§

Corinne Rancurel,† Daniel B. Leznoff,† Jean-Pascal Sutter,*,† Philippe Guionneau,† Daniel Chasseau,† Janis Kliava,‡ and Olivier Kahn*,†

Laboratoire des Sciences Moléculaires, Institut de Chimie de la Matière Condensée de Bordeaux, UPR CNRS No. 9048, 33608 Pessac, France, and Centre de Physique Moléculaire Optique et Hertzienne, UMR Université Bordeaux I-CNRS, 351, cours de la Libération, 33405 Talence, France

Received August 11, 1999

Introduction

The study of discrete multispin systems is an important facet of molecular magnetism.[1] It has been shown that both the nature of the spin carriers and their topology determine the overall magnetic behavior of multispin complexes. The combination of radical-containing ligands and paramagnetic metals, i.e., the "metallo-organic radical approach",[2] has led to a wide variety of discrete complexes with various topologies,including large rings,[3,4] butterfly arrangements,[5] tetrahedra, and octahedra.[6] Many of these nonlinear compounds exhibit antiferromagnetic interactions, leading to overall ferrimagnetic or spin-frustration magnetic behavior. Less common are isolated complexes which incorporate *both* antiferromagnetic and ferromagnetic interactions.[7] We hereby present such a compound, of formula {[*o*PONit]MnCl(μ-Cl)}$_2$ where oPONit stands for (*o*-nitronyl nitroxide-phenyl)diphenylphosphine oxide. This compound is a *linear*, four-spin system with a ground state spin of $S = 4$ showing distinctly both basic types of magnetic interactions.

Experimental Section

General Procedures. Unless otherwise stated, all manipulations were performed in air using purified solvents. Under a nitrogen atmosphere, EtOH was dried over Mg, Et_2O over Na/benzophenone, and MeCN over P_2O_5 and all were distilled prior to use. The nitronyl nitroxide-substituted triphenylphosphine oxide ligand **1** was prepared as previously described.[8] All other reagents were obtained from commercial sources and used as received. Infrared spectra were collected on a Perkin-Elmer FT-IR Pergamon 1000 spectrometer. ESR spectra were collected on a Bruker EMX spectrometer operating in the X-band (9.46 GHz) equipped with an Oxford ESR-900 flowing-helium cryostat (4.2−300 K) controlled by an Oxford ITC4 temperature control unit. Elemental analyses were conducted by the central CNRS microanalysis service (Lyon). Magnetic susceptibility data were collected in the 2−300 K range using a SQUID MPMS-5S magnetometer at 1000 Oe field strength. The data were corrected for the diamagnetism of the constituent atoms.

Table 1. Summary of Crystallographic Data

	2
formula	$C_{54}H_{58}Cl_4Mn_2N_6O_6P_2$
fw	1200.68
space group	$P\bar{1}$
a, Å	10.234(2)
b, Å	10.438(2)
c, Å	13.853(2)
α, deg	81.12(1)
β, deg	79.63(1)
γ, deg	78.42(1)
V, Å^3	1415(1)
Z	2
ρ_{calc}, g/cm^3	1.409
T, K	293
μ, mm^{-1}	0.745
R1, wR2 ($I \geq 2\sigma(I)$)[a]	0.047, 0.125
R1, wR2 (all data)[a]	0.070, 0.137

[a] Function minimized $\sum w(|F_o^2 - F_c^2|)^2$ where $w^{-1} = \sigma^2(F_o^2)$, $R1 = \sum||F_o| - |F_c||/\sum|F_o|$, $wR2 = (\sum w(F_o^2 - F_c^2)^2/\sum w(F_o^2)^2)^{1/2}$.

Synthesis of Bis-{[(*o*-nitronyl nitroxide-phenyl)diphenylphosphine oxide]MnCl(μ-Cl)}, {[*o*PONit]MnCl(μ-Cl)}$_2$ (2). A solution of anhydrous $MnCl_2$ (0.014 g, 0.11 mmol) in 4 mL of absolute ethanol was prepared under nitrogen. To this was added phosphine oxide **1** (0.050 g, 0.11 mmol) directly as a solid, and the resulting solution was heated to 35 °C for 30 min. The ethanol was removed in vacuo, and the paste obtained was redissolved in 2 mL of MeCN. Slow diffusion of Et_2O into this red solution produced small crystals of {[*o*PONit]-MnCl(μ-Cl)}$_2$ (**2**). Yield: 0.058 g (90%). Anal. Calcd for $C_{50}H_{52}N_4$-$Cl_4Mn_2O_6P_2 \cdot 2CH_3CN$: C, 54.02; H, 4.86; N, 6.99; Mn, 9.15. Found: C, 53.55; H, 4.78; N, 6.88; Mn, 8.74. IR (KBr): 1438 (s), 1363 (s, N−O), 1173 (s, P═O), 1139 (s), 1119 (s), 722 (s), 550 (m) cm^{-1}. Intense orange crystals suitable for X-ray analysis were obtained by slow diffusion of Et_2O into a MeCN solution of **2**, conducted in a 150 mm long tube of 1.5 mm diameter.

X-ray Crystallographic Analysis. The title compound crystallizes as irregular plates. The X-ray diffraction quality of a crystal of approximate dimensions 0.40 × 0.35 × 0.16 mm^3 was checked by the Weissenberg method. A full data collection was performed at 295 K on a Nonius CAD-4 diffractometer with Mo Kα radiation (0.71069 Å). The diffracted intensities were collected within the range $2.00° < \theta < 28.00°$ using $\omega - {}^2/_3\theta$ scans. No deviation was observed during the data collection on the intensity of three reference reflections. A total of 8242 reflections were measured, of which 6232 are independent ($R_{int} = 5.0\%$). The computing data reduction was performed using the Nonius software. An absorption correction based on ψ scans was applied ($T_{min} = 0.892$, $T_{max} = 1.000$). The crystal structure was solved with Patterson and direct methods using the SHELX-97 package.[9] The same software was used to perform a least-squares refinement ($R_{final} = 0.048$) of the atomic parameters (339). Hydrogen atoms were placed in theoretical positions. The asymmetric unit contains half a molecule that lie on a center of inversion and a CH_3CN solvent molecule. Crystallographic data appear in Table 1. Selected bond lengths and angles are found in Table 2.

§ This paper is dedicated to the memory of Professor Olivier Kahn who passed away suddenly on December 8, 1999.

† Institut de Chimie de la Matière Condensée de Bordeaux.

‡ UMR Université Bordeaux I-CNRS.

(1) Kahn, O. *Molecular Magnetism*; VCH: Weinheim, 1993.
(2) Caneschi, A.; Gatteschi, D.; Sessoli, R.; Rey, P. *Acc. Chem. Res.* **1989**, *22*, 392.
(3) Görlitz, G.; Hayamizu, T.; Itoh, T.; Matsuda, K.; Iwamura, H. *Inorg. Chem.* **1998**, *37*, 2083.
(4) Caneschi, A.; Gatteschi, D.; Laugier, J.; Rey, P.; Sessoli, R.; Zanchini, C. *J. Am. Chem. Soc.* **1988**, *110*, 2795.
(5) Tanaka, M.; Matsuda, K.; Itoh, T.; Iwamura, H. *Angew. Chem., Int. Ed. Engl.* **1998**, *37*, 810.
(6) Fegy, K.; Sanz, N.; Luneau, D.; Belorizky, E.; Rey, P. *Inorg. Chem.* **1998**, *37*, 4518.
(7) Ruiz, R.; Lloret, F.; Julve, M.; Faus, J.; Munoz, M. C.; Solans, X. *Inorg. Chim. Acta* **1998**, *268*, 263.
(8) Rancurel, C.; Sutter, J.-P.; Kahn, O.; Guionneau, P.; Bravic, G.; Chasseau, D. *New J. Chem.* **1997**, *21*, 275.
(9) Sheldrick, G. *Software for crystallography, SHELX-97*; University of Göttingen, Göttingen, 1997.

10.1021/ic9909678 CCC: $19.00
Published on Web 03/10/2000

Table 2. Selected Bond Lengths (Å) and Angles (deg) for {[*o*PONit]MnCl(μ-Cl)}$_2$ (**2**)

Mn(1)−Cl(2)	2.4356(8)	Mn(1)−O(1)	2.0989(16)
Mn(1)−Cl(2a)	2.5119(8)	Mn(1)−O(2)	2.1401(18)
Mn(1)−Cl(1)	2.3402(9)	N(1)−O(2)	1.283(2)
Mn(1)−Mn(1a)	3.626(1)	N(2)−O(3)	1.261(3)
P(1)−O(1)	1.4926(7)		
Cl(2a)−Mn(1)−Cl(2)	85.74(3)	Cl(1)−Mn(1)−O(1)	108.92(5)
Mn(1)−Cl(2)−Mn(1a)	94.26(3)	Cl(1)−Mn(1)−O(2)	100.69(7)
Cl(2)−Mn(1)−O(1)	89.42(5)	P(1)−O(1)−Mn(1)	134.45(10)
Cl(2a)−Mn(1)−O(2)	158.53(7)	N(1)−O(2)−Mn(1)	129.58(15)

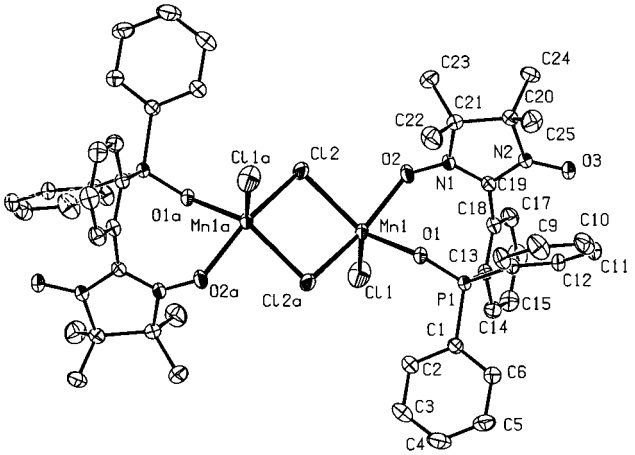

Figure 1. Molecular structure (ORTEP, 30% ellipsoids) and numbering scheme for {[*o*PONit]MnCl(μ-Cl)}$_2$ (**2**).

Results and Discussion

Synthesis and Structure of {[*o*PONit]MnCl(μ-Cl)}$_2$ (2). Addition of the nitronyl nitroxide-substituted phosphine oxide ligand [*o*PONit] (**1**) to anhydrous $MnCl_2$ followed by MeCN/Et_2O crystallization gives {[*o*PONit]MnCl(μ-Cl)}$_2$ (**2**) in high yield (eq 1). The $\nu_{P=O}$ absorption band in the infrared region shifts from 1197 cm^{-1} in the free ligand to 1174 cm^{-1} upon metal complexation.

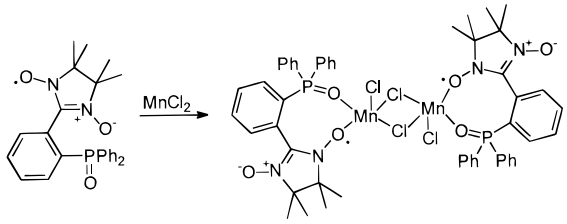

1 **2** (1)

The structure, shown in Figure 1, reveals **2** to be a binuclear manganese(II) complex containing two [*o*PONit]MnCl units bridged by two additional chloride ligands. Phosphine oxide **1** acts as a bidentate, chelating ligand via the oxygen atoms of the P═O and N−O moieties. Hence the Mn(II) center is pentacoordinate and in a tetragonal pyramidal geometry. There are only two other crystallographically characterized Mn(II) complexes with this combination of bridging and terminal chloride ligands: {[2,2′-diquinolyl]MnCl(μ-Cl)}$_2$[10] and {[diphenylformamidinate]$_2$MnCl(μ-Cl)}$_2$.[11] The Mn(1)−Cl(2), Mn(1)−Cl(2a), and Mn(1)−Cl(1) bond lengths of 2.4356(8), 2.5119(8), and 2.3402(9) Å in **2** for the two bridging and one terminal Mn−Cl, respectively, are comparable to those found in the aforementioned complexes. Note that the Mn(1)−Mn(1a) distance of 3.626(1) Å is too long to consider the presence of a metal−metal bond.[12]

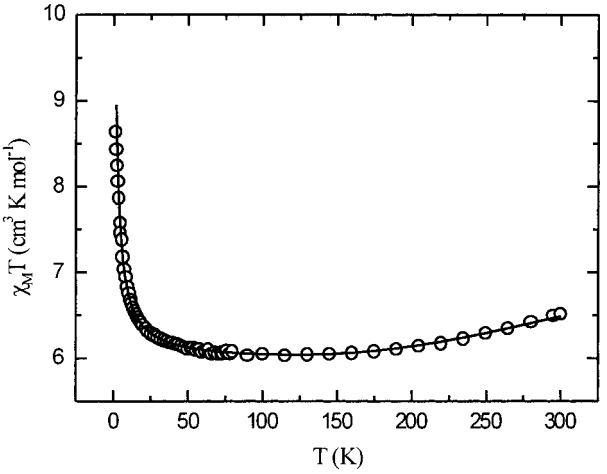

Figure 2. Temperature dependence of $\chi_M T$ for **2**. The solid line represents the calculated best fit to the experimental data as described.

The N−O bond lengths of 1.261(3) and 1.283(2) Å for noncoordinated and coordinated N−O groups, respectively, are significantly different, as is usually observed,[13] and can be compared to values of 1.269(4) and 1.280(4) Å in the free ligand.[8] The Mn(1)−O(2) bond length of 2.1401(18) Å is similar to other Mn(II)−aminoxyl bonds.[14] The Mn(1)−O(1) and P(1)−O(1) bond lengths of 2.0989(16) and 1.4926(7) Å are slightly longer than the 2.069(6) and 1.488(6) Å found in $MnCl_2$-$(OPPh_3)_2$.[15] The P═O bond length in **1** is 1.473(3) Å; this has substantially lengthened upon coordination. This effect is also visible as a lowering of the $\nu_{P=O}$ absorption band in the infrared region, as described above. Another structural change in the ligand upon coordination is the exacerbation of the steric twist in the ligand structure. The dihedral angle between the nitronyl nitroxide fragment and the phenyl ring to which it is bound is 76.6° in **2** compared to 62.8° in free ligand **1**.[8] There are no significant intermolecular contacts in the structure of **2**. The nearest intermolecular N−O···N−O contact is 6.314 Å. Hence, each dimeric unit can be considered to be magnetically isolated.

Magnetic Behavior. The variable-temperature magnetic susceptibility of **2** is shown in Figure 2 as a plot of $\chi_M T$ vs T. At 300 K $\chi_M T$ is equal to 6.5 cm^3 K mol^{-1}, a value much lower than that expected for two non-interacting $S = {}^5/_2$ Mn(II) centers and two $S = {}^1/_2$ radicals ($\chi_M T$ = 9.5 cm^3 K mol^{-1}) but close to the $\chi_M T$ value for two uncorrelated $S = 2$ systems ($\chi_M T$ = 6.0 cm^3 K mol^{-1}). It is well-known that nitroxide radicals directly bound to Mn(II) centers exhibit strong antiferromagnetic coupling; hence an effective spin state of $S = 2$ for each Mn−O−N radical pair is reasonable.[13,16] Indeed, as the temperature is lowered to 170 K, $\chi_M T$ gradually decreases to reach a plateau value of 6.0 cm^3 K mol^{-1}, consistent with two non-interacting $S = 2$ spin systems; this remains stable until approximately 70 K. Below this temperature, $\chi_M T$ increases in value to reach 8.7 cm^3 K mol^{-1} at 2 K.

In **2** the nitronyl nitroxide radicals are nonbridging and the two radical moieties are intra- and intermolecularly well-

(10) Sinn, E. *J. Chem. Soc., Dalton Trans.* **1976**, 162.
(11) Arnold, D. I.; Cotton, F. A.; Maloney, D. J.; Matonic, J. H.; Murillo, C. A. *Polyhedron* **1997**, *16*, 133.
(12) Vahrenkamp, H. *Angew. Chem., Int. Ed. Engl.* **1978**, *17*, 379.
(13) Caneschi, A.; Gatteschi, D.; Rey, P. *Prog. Inorg. Chem.* **1991**, *39*, 331.
(14) Nakatsuji, S.; Anzai, H. *J. Mater. Chem.* **1997**, *7*, 2161.
(15) Tomita, K. *Acta Crystallogr. C* **1985**, *C41*, 1832.
(16) Fegy, K.; Luneau, D.; Belorizky, E.; Novak, M.; Tholence, J.-L.; Paulsen, C.; Ohm, T.; Rey, P. *Inorg. Chem.* **1998**, *37*, 4524.

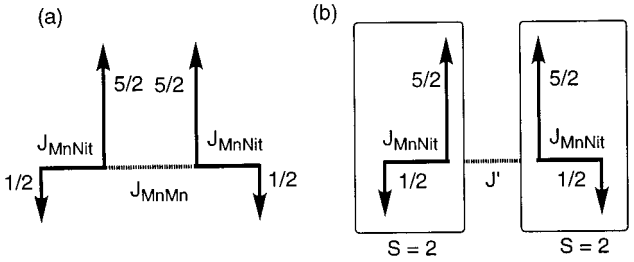

Figure 3. (a) Spin diagram with ferromagnetic interaction J_{MnMn} between two $S = {}^5/_2$ Mn(II) centers. (b) Spin diagram assuming $|J_{MnNit}| \gg |J_{MnMn}|$, with ferromagnetic interaction J' between two $S = 2$ effective spin units (Mn−aminoxyl).

separated from each other. This generates a linear spin topology. From a magnetic point of view, this linear four-spin system can be represented as shown in Figure 3a. The interactions between the $S = {}^1/_2$ and $S = {}^5/_2$ units are strong and detectable at high temperatures ($T > 70$ K) while the interaction between the two Mn $S = {}^5/_2$ units is very small, and only detectable in the low-temperature range ($T < 70$ K). Between 70 and 170 K, the system obeys the Curie law for two isolated $S = 2$ states. Below 70 K, the interaction between the two Mn(II) centers becomes significant and must be taken into account. The spin Hamiltonian that fully describes the situation shown in Figure 3a is given in eq 2, where J_{MnNit} and J_{MnMn} characterize the Mn−radical and Mn−Mn interactions, respectively; all other terms have their usual meanings. The solution to this equation, while tractable, is quite complex, involving a spin degeneracy of 144 ($2 \times 6 \times 6 \times 2$). However, the nature of the experimental data allows us to make some simplifications to the above equation and still interpret the magnetic data in a meaningful fashion.

$$H = -J_{MnNit}(\mathbf{S_{Mn1}}\cdot\mathbf{S_{Nit1}} + \mathbf{S_{Mn2}}\cdot\mathbf{S_{Nit2}}) - J_{MnMn}\mathbf{S_{Mn1}}\cdot\mathbf{S_{Mn2}} + [g_{Mn}(\mathbf{S_{Mn1}} + \mathbf{S_{Mn2}}) + g_{Nit}(\mathbf{S_{Nit1}} + \mathbf{S_{Nit2}})]\beta\mathrm{H} \quad (2)$$

It is quite clear from the $\chi_M T$ curve that $|J_{MnNit}| \gg |J_{MnMn}|$ (Figure 3a). This leads to the key feature of the experimental curve: between 70 and 170 K, Curie law behavior for two noninteracting $S = 2$ states is observed. Hence, each Mn−aminoxyl unit can be treated as an effective $S = 2$ spin center from a magnetic point of view as only the $S = 2$ state of each pair is populated at 70 K. The effects of the strong antiferromagnetic interactions and weaker ferromagnetic interaction are well separated in the $\chi_M T$ curve. As a result, the intramolecular ferromagnetic interaction could instead be described as occurring between the two $S = 2$ antiferromagnetically coupled Mn−O−N units, using a parameter J' (Figure 3b). That is, J_{MnMn} is defined in the basis set $|S_{Nit1}, S_{Mn1}, S_{Nit2}, S_{Mn2}, M_{Nit1}, M_{Mn1}, M_{Nit2}, M_{Mn2}\rangle$ and J' in $|S_{NitMn1}, S_{NitMn2}, M_{NitMn1}, M_{NitMn2}, S_{Nit1}, S_{Mn1}, S_{Nit2}, S_{Mn2}\rangle$. S_{NitMn1} and S_{NitMn2} are the quantum numbers associated with the spin operators $\mathbf{S_{NitMn1}} = \mathbf{S_{Nit1}} + \mathbf{S_{Mn1}}$ and $\mathbf{S_{NitMn2}} = \mathbf{S_{Nit2}} + \mathbf{S_{Mn2}}$, respectively. It is easy to show that $J' = (7/6)^2 J_{MnMn}$. This perturbation of the two $S = 2$ states generates the energy level diagram shown in Figure 4 and is only valid in the case where $|J_{MnNit}| \gg |J'|$. The left and right sides represent the non-interacting $S = 2$ states composed of the Mn(II)−aminoxyl units and their first excited $S = 3$ states, with an energy level separation of $3J_{MnNit}$. The center of the diagram represents the total interacting system, where J' characterizes the exchange interaction between the two $S = 2$ units. The interactions between the $S = 2$ and $S = 3$ states and between $S = 3$ excited states can be neglected.

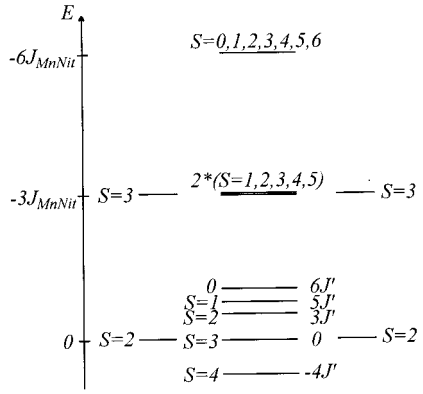

Figure 4. Energy level diagram for **2** based on the spin diagram in Figure 3b.

The ground state of the system is thus $S = 4$, corresponding to the ferromagnetic interaction between two $S = 2$ states. The energy level diagram shows that the first excited state, $S = 3$, of the whole system is $4J'$ above the ground-state $S = 4$. Assuming $g_{Mn} = g_{Nit} = 2$ and using the Van Vleck equation results in eq 3 for the magnetic susceptibility of the system,

$$\chi_M = \frac{Ng^2\beta^2}{kT}\left[\frac{28 + 60e^{4J'/kT} + 10e^{-3J'/kT} + 2e^{-5J'/kT} + 420e^{3J/kT} + 392e^{6J/kT}}{7 + 9e^{4J'/kT} + 5e^{-3J'/kT} + 3e^{-5J'/kT} + e^{-6J'/kT} + 70e^{3J/kT} + 49e^{6J/kT}}\right] \quad (3)$$

where $J = J_{MnNit}$, J' is defined above, and all other terms have their usual meaning. The calculated fit of the experimental data using eq 3 is shown as a solid line in Figure 2. Fitting over the entire temperature range yields parameter values of $J = -189$ cm^{-1} and $J' = +0.49$ cm^{-1}. Note that the $\chi_M T$ value of 8.7 cm^3 K mol^{-1} at 2 K implies that the $S = 4$ ground state is not completely populated at this temperature ($\chi_M T = 10$ cm^3 K mol^{-1} for $S = 4$).

Ferromagnetic interactions between two $S = {}^5/_2$ Mn(II) centers via chloride bridges is precedented but has not been studied in detail. {[2,2′-Diquinolyl]MnCl(μ-Cl)}$_2$ shows ferromagnetic interactions leading to a ground state of $S = 5$, but the magnetic properties were not reported in detail.[10] The magnetic behavior of {[diphenylformamidinate]$_2$MnCl(μ-Cl)}$_2$ was not reported.[11] A high-spin Cr(II) chloride-bridged dimer ($2 \times S = 2$), which would also be analogous to **2**, is weakly antiferromagnetically coupled.[17] Of course, magnetically active chloride-bridged systems are well-known in general. The angular dependence of the strength and nature of the magnetic coupling in M(μ-X)M systems has been studied in detail for Cu^{II}_2 and Cr^{III}_2 systems.[1] Geometry and topology obviously play important roles in determining the nature of the chloride-mediated coupling: [Cp*RuCl(μ-Cl)]$_2$ has a geometry similar to that of **2** and also exhibits weak ferromagnetic coupling[18] while both [(MeCp)MnCl(PEt$_3$)]$_2$[19] and polymeric [C_5H_5NH][$MnCl_3$]·H_2O.[20] (Mn(II) systems) show antiferromagnetic interactions.

EPR Spectrum. The powder X-band EPR spectrum was recorded at various temperatures down to 4 K. Surprisingly, below 100 K, the spectrum remains essentially unchanged,

(17) Fryzuk, M. D.; Leznoff, D. B.; Rettig, S. J.; Thompson, R. C. *Inorg. Chem.* **1994**, *33*, 5528.
(18) Koelle, U.; Lueken, H.; Handrick, K.; Schilder, H.; Burdett, J. K.; Balleza, S. *Inorg. Chem.* **1995**, *34*, 6273.
(19) Köhler, F. H.; Hebendanz, N.; Müller, G.; Thewalt, U.; Kanellakopulos, B.; Klenze, R. *Organometallics* **1987**, *6*, 115.
(20) Caputo, R.; Willet, R. D.; Morosin, B. *J. Chem. Phys.* **1978**, *69*, 4976.

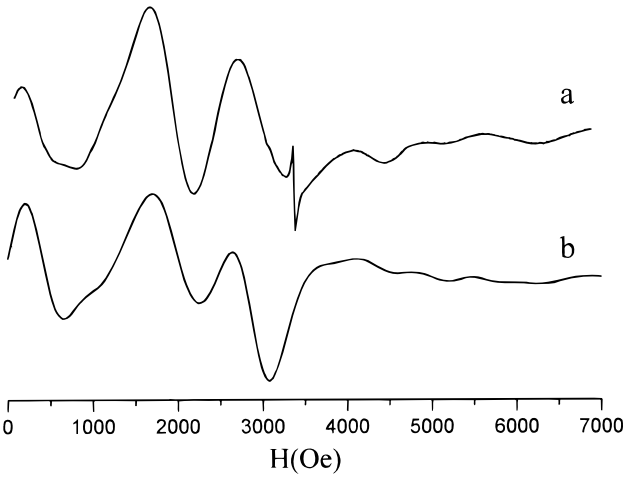

Figure 5. (a) Observed powder X-band EPR spectrum for **2** at 10 K. (b) Simulated powder EPR spectrum of the $S = 2$ state.

without any detectable modification of the relative intensities of the peaks. Moreover, this spectrum is characteristic of an $S = 2$ state with a zero-field splitting axial parameter smaller than the incident quantum. A typical spectrum, recorded at 10 K, is shown in Figure 5. This spectrum is rather similar to those obtained for two other Mn(II) derivatives of nitronyl-nitroxide phosphine oxide, namely, the *p*- and *o*-(nitronyl-nitroxide-phenyl)diphenylphosphine oxide.[21] The very weak ferromagnetic interaction between the Mn(II) ions revealed by the magnetic properties seems not to influence the powder EPR spectrum. This might be due to the fact that the total Zeeman splitting of the $S = 2$ state is ca. 1 cm^{-1}, which is larger than J'. This spectrum is governed by the Mn(II)−radical antiferromagnetic interaction which gives rise to an $S = 2$ state for each [*o*PONit]-Mn moiety. The experimental EPR spectrum was computer simulated using a laboratory-developed computer program for paramagnetic centers described by the spin Hamiltonian in eq 4 where $S = 2$ and all symbols have their usual meaning.

$$H = \beta \mathrm{H}\cdot\mathbf{g}\cdot\mathbf{S} + \mathrm{D}[\mathbf{S_z}^2 - (1/3)S(S+1)] + E(\mathbf{S_x}^2 - \mathbf{S_y}^2) \quad (4)$$

The simulation program carries out a repeated search for resonance magnetic fields $H_r(D,E,\vartheta,\varphi)$ yielding the energy-level separations that match the microwave quantum value, ϑ and φ being the polar and azimuthal angles of the static magnetic field vector H in the *x*, *y*, *z* set of axes. The random orientation of the paramagnetic centers is accounted for by a Monte Carlo search for sin ϑ and φ values using the RANMAR Fortran code described in ref 22 to generate pseudorandom numbers. Besides, the program takes into account a possibility of a (correlated) Gaussian distribution in the D and E values with the density

$$P(D,E) = \frac{1}{2\pi\Delta D\Delta E\sqrt{1-\rho^2}} \exp\left\{-\frac{1}{2(1-\rho^2)}\left[\left(\frac{D-\bar{D}}{\Delta D}\right)^2 - 2\rho\frac{(D-\bar{D})(E-\bar{E})}{\Delta D\Delta E} + \left(\frac{E-\bar{E}}{\Delta E}\right)^2\right]\right\} \quad (5)$$

with $\bar{D}$, $\bar{E}$ the mean values and ΔD, ΔE the root-mean-square deviations of the corresponding parameters, ρ being the correlation coefficient. The Gaussian distribution is implemented by summing up 12 random numbers supplied by the RANMAR generator. The derivative-of-absorption powder spectra are generated in accordance with eq 6 where $W(D,E,\vartheta,\varphi)$ is the transition intensity calculated using the eigenvectors of H and averaged over all directions of the microwave magnetic field and $F[H - H_r(D,E,\vartheta,\varphi),\Delta H]$ is the intrinsic line shape which was chosen as a Gaussian derivative with a peak-to-peak width ΔH. The parameters in eqs 4 and 5 were found as $g = 2.00$ (**g** tensor isotropic), $\bar{D} = 0.23$ cm^{-1}, $\bar{E} = 0.028$ cm^{-1}, $\Delta D = 0.04$ cm^{-1}, $\Delta E = 0.003$ cm^{-1}, $\Delta H = 200$ Oe, and $\rho = 0.0$. The simulated spectrum is also shown in Figure 5. Taking into account a possible anisotropy in the g values could not improve the fit. A distribution of zero-field splitting parameters at the first view does not seem to be in line with the concept of perfectly defined molecules. Perhaps, to some extent, it compensates the absence of terms *quartic* in S and/or of high-spin Zeeman terms[23] in the spin Hamiltonian (eq 4).

$$P(H) = \int_{-\infty}^{+\infty}\int_0^{D/3}\int_0^{2\pi}\int_0^{\pi} P(D,E)W(D,E,\vartheta,\varphi)F[H - H_r(D,E,\vartheta,\varphi),\Delta H]\sin\vartheta\,\mathrm{d}\vartheta\,\mathrm{d}\varphi\,\mathrm{d}E\,\mathrm{d}D \quad (6)$$

Conclusion

This Note is devoted to a new compound incorporating a nitronyl nitroxide-substituted phosphine oxide. In contrast with the first two compounds of this kind recently reported,[21] the title compound exhibits both ferro- and antiferromagnetic interactions. A four-spin system containing the same four spin carriers as in **2** (two Mn(II) and two nitronyl nitroxide radicals) was recently reported in which the *diamond-like* topology led to a spin-frustrated complex.[5] A simple rearrangement of the four spin elements into the *linear* topology of compound **2** generates completely different magnetic behavior. In the near future, we will explore further the rich chemistry of these new nitronyl nitroxide-substituted phosphine oxide ligands.

Acknowledgment. Financial support was provided by NSERC of Canada in the form of a postdoctoral fellowship (to D.B.L.) and by the TMR Research Network ERBFMRX-CT980181 of the European Union, entitled "Molecular Magnetism, from Materials toward Devices".

Supporting Information Available: One X-ray crystallographic file, in CIF format. This material is available free of charge via the Internet at http://pubs.acs.org.

IC9909678

(21) Rancurel, C.; Leznoff, D. B.; Sutter, J.-P.; Golhen, S.; Ouahab, L.; Kliava, J.; Kahn, O. *Inorg. Chem.* **1999**, *38*, 4753.
(22) James, F. *Comput. Phys. Commun.* **1990**, *60*, 329.
(23) McGavin, D. G.; Tennant, W. C.; Weil, J. A. *J. Magn. Reson.* **1990**, *87*, 92.